Polymer 55 (2014) 4738–4747

Contents lists available at ScienceDirect

Polymer

journal homepage: www.elsevier.com/locate/polymer

The role of linked phospholipids in the rubber-filler interaction in carbon nanotube (CNT) filled natural rubber (NR) composites

H.H. Le [a, b, *], S. Abhijeet [c], S. Ilisch [d], J. Klehm [e], S. Henning [e], M. Beiner [e], S.S. Sarkawi [f], W. Dierkes [g], A. Das [a], D. Fischer [a], K.-W. Stöckelhuber [a], S. Wiessner [a, h], S.P. Khatiwada [i], R. Adhikari [i], T. Pham [j], G. Heinrich [a, h], H.-J. Radusch [c]

[a] Leibniz-Institut für Polymerforschung Dresden, Germany
[b] Polymer Service GmbH Merseburg, Merseburg, Germany
[c] Martin-Luther-Universität Halle-Wittenberg, Halle (Saale), Germany
[d] Styron Deutschland GmbH, D-06258 Schkopau, Germany
[e] Fraunhofer IWM, Walter-Hülse-Str. 1, D-06120 Halle (Saale), Germany
[f] Malaysian Rubber Board, RRIM Research Station, Sg. Buloh, 47000 Selangor, Malaysia
[g] University of Twente, Elastomer Technology and Engineering, P.O. Box 217, 7500 AE Enschede, The Netherlands
[h] Technische Universität Dresden, Germany
[i] Central Department of Chemistry, Tribhuvan University, Kirtipur, Kathmandu, Nepal
[j] Borealis Polyolefine GmbH, A-4021 Linz, Austria

ARTICLE INFO

Article history:
Received 27 February 2014
Received in revised form
12 June 2014
Accepted 22 July 2014
Available online 1 August 2014

Keywords:
Non-rubber components
Carbon nanotubes
Filler wetting

ABSTRACT

The aim of the present work is to evidence the role of the linked phospholipids of natural rubber (NR) in the rubber-carbon nanotube (CNT) interactions in rubber composites. Three rubbers namely NR, deproteinized NR (DPNR) and a synthetic rubber isoprene (IR) were used as matrix for CNTs. The selective wetting of CNTs in miscible NR/IR and DPNR/IR blends was investigated by means of the modified *wetting concept* based on Fourier transformed infrared (FTIR) analysis of the rubber-filler gel of blends. It revealed that the surface of CNTs is entirely wetted by NR or DPNR molecules, respectively, but not by IR. This result emphasizes that proteins do not influence the affinity between NR and CNTs, while the linked phospholipids interact with CNT surface through cation-π linkage. This linkage acts as anchor point supporting NR molecules to wet CNT surface effectively. The modified *wetting concept* can be used for characterization of selective wetting of different fillers in blends consisting of miscible rubber components.

1. Introduction

Natural rubber (NR) is considered as one of the most important bio-based polymers possessing excellent chemical and physical properties, such as outstanding elasticity and flexibility. It is widely used in various areas such as tyres, sport articles, sealing materials and dairy rubber item [1], for instance, about 70% of rubber consumed in tire industry is from NR. Recently, nanofillers have been added into tire tread compounds in order to impart them some functionalities like gas barrier, flammability resistance, electrical conductivity, polymer blend compatibility [2–7]. Among nanofillers carbon nanotubes (CNTs) are of high interest in polymer materials because of their high aspect ratio, high surface area available for stress transfer as well as their exceptionally high Young's modulus and excellent electrical and thermal properties [7]. A number of works [8–12] has reported on CNT/NR nanocomposites regarding preparation techniques and vulcanization characteristics as well as physical, mechanical and thermal properties. Apart from that, NR has often been blended with different synthetic rubbers in order to improve abrasion resistance and oxidative stability of tires [13–19]. Boonmathisud et al. [14,15] prepared CNT filled NR/styrene butadiene rubber (SBR) and NR/carboxylated SBR (XSBR) blends using latex mixing method. The results revealed that nanofiller improved tensile strength, modulus, dynamic mechanical properties and thermal stability but reduced the elongation at break. Kueseng et al. [16,17] used masterbatch mixing method for preparation of CNT filled NR/nitrile butadiene

* Corresponding author. Leibniz-Institut für Polymerforschung Dresden, Dresden, Germany.
E-mail address: le-haihong@ipfdd.de (H.H. Le).

http://dx.doi.org/10.1016/j.polymer.2014.07.043
0032-3861/

rubber (NBR) blends. The stronger reinforcing efficiency was reached when the masterbatch prepared by the pre-dispersing method was utilized. In addition, the volume resistivity of the masterbatch blends was lower than that of the corresponding statistic blends by about 2 orders of magnitude. The effect of machine direction and transverse direction on the orientation of CNTs and the related mechanical and electrical properties of the blends was also elucidated. Moreover, the solvent transport and electrical properties as well as compatibilising effects of the CNT filled NR/NBR blends were also investigated by Thomas et al. [18] and Yan et al. [19]. Improvement of the properties of nanocomposites in these mentioned works was discussed by taking into consideration the great aspect ratio and specific surface area of CNTs. It is generally accepted that a good dispersion and homogeneous wetting of CNTs in the polymer blends are essential of composite properties. Up to date, however, the selective wetting of CNTs in rubber blends has not been characterized systematically so far. Recently, in our previous works [20,21] the selective localization of CNTs in binary SBR/NR blends and ternary SBR/BR/NR and SBR/NBR/NR blends was investigated. It was found that NR molecules dominantly wet CNT surface, while SBR and BR nearly have no contact with CNTs. The non-polar NR is also able to compete with the polar rubber NBR with respect to the CNT wetting. A possible explanation could be related to the effect of the non-rubber components presented in NR, which are believed to enhance the interaction between NR and CNTs.

In the present work, in order to identify the non-rubber component which is mainly responsible for the strong rubber-filler interaction in CNT/NR nanocomposites we proposed a new strategy for a direct comparison between different rubbers regarding the affinity to CNTs. Accordingly, CNTs were mixed into two blends consisting of NR and isoprene (IR) as well as deproteinized natural rubber (DPNR) and IR, respectively. IR is a “clean” rubber with isoprene units in the backbone without any functional groups. NR is made up by isoprene units and phospholipids and proteins linked to two terminals of its molecule. DPNR contains only phospholipids at a terminal, because proteins were almost removed by a deproteinization process. The selective wetting of CNTs by different rubber molecules was quantitatively characterized by means of the *wetting concept*. Based on the selective wetting of CNTs the rubber-CNT affinity can be discussed and the role of non-rubber components in NR can be distinguished.

2. Experimental

2.1. Materials and mixture preparation

Natural rubber (NR) (Standard Malaysian Rubber (SMR 10), Weber & Schaer GmbH) with a nitrogen content of 0.6 wt% and deproteinized natural rubber (DPNR) (Pureprena, Malaysian Rubber Board) with a nitrogen content of 0.08 wt% as well as synthetic polyisoprene (IR) (Cariflex JR 309, Shell Chemical Co.) with 95 wt% cis-1,4 isoprene units were used as rubber matrix. NR and DPNR were masticated by means of a two-roll mill in order to reduce their Mooney viscosity to the range of IR. Multi-walled carbon nanotubes (CNTs) (Nanocyl™ NC7000, Nanocyl S.A., Belgium) were used as filler. According to the provider Nanocyl possesses an average diameter of 10 nm and a broad length distribution with several nanotubes up to 10 μm. The amorphous carbon content is about 3 wt% and an impurity of 10 wt% is detected as metal oxide.

For preparation of CNT filled compounds and blends an internal mixer (Rheocord 300p, ThermoHaake) was used by keeping the following mixing conditions: initial chamber temperature T_A of 50 °C, rotor speed of 75 rpm and fill factor of 0.68. The criterion for a choice of mixing conditions used in the present work is to obtain a good CNT dispersion, and the development of CNT dispersion must be slow enough for taking out the sample along the mixing time for further investigations.

A conductivity sensor system was installed in the chamber of the internal mixer to measure the electrical signal of the conductive mixtures. Two statistic blends were prepared by mixing 5 phr CNTs into 50/50 NR/IR and 50/50 DPNR/IR blend. Two masterbatch blends were also prepared by mixing IR/CNT masterbatch with the fresh NR or DPNR. The compositions of masterbatch blends are kept similar to that of statistic blends. For an effective dispersion of CNTs in rubber matrix an ethanol-assisted mixing process (*wet mixing*) according to our previous work [20,21] was applied, however, no further non-ionic surfactant was used for stabilizing the nanotubes in the ethanolic medium. CNTs were first wetted with a certain amount ethanol to a paste. Then, it was added into the mixing chamber with rubber for preparation of the composites and masterbatches. Ethanol was entirely vaporized during the mixing process. A ratio ethanol/CNT of 3.7 was chosen for a good dispersion of CNTs.

2.2. Experimental determination of filler wetting in rubber compounds and blends

For the investigation of the rubber-filler gel of the compounds and blends, for example from NR and IR, 0.1 g of each raw mixture was stored for seven days in 100 ml cyclohexane at room temperature. The rubber-filler gel was taken out and dried up to a constant mass. The rubber content in the gel L^{NR} and L^{IR} as well as $L^{B(NR/IR)}$ as a measure for the wetting behavior of CNT surface by NR and IR as well as NR/IR blend, respectively, is determined according to Eq. (1) [22].

$$L = \frac{m_2 - m_1 \cdot c_{CNT}}{m_2} \tag{1}$$

The mass m_1 is corresponding to the rubber compound before extracting. m_2 is the mass of the rubber-filler gel, which is the sum of the undissolvable rubber part and the mass of CNTs. c_{CNT} is the mass concentration of CNTs in the single rubber mixture or binary blends. For NR/IR blend the rubber layer $L^{B(NR/IR)}$ is the rubber part in the rubber-filler gel and consists of two contributions according to Eq. (2).

$$L^{B(NR/IR)}(t) = L^{B(NR)}(t) + L^{B(IR)}(t) \tag{2}$$

$L^{B(NR)}$ and $L^{B(IR)}$ can be determined by means of a calibration curve. For creation of the calibration curve, blends with different NR/IR mass ratios were prepared and investigated by FTIR according to the procedure described in our previous work [22]. FTIR spectral were recorded by use of an FTIR spectrometer S2000 (Perkin Elmer) equipped with a diamond single Golden Gate ATR cell (Specac). The peaks at 1376 cm^{-1} and 888 cm^{-1} were used for calculation of the ratio of the surface under peak A^{NR}/A^{IR}. The correlation between the A^{NR}/A^{IR} ratio and the given NR/IR mass ratio can be established, and based on this correlation the ratio $L^{B(NR)}/L^{B(IR)}$ of the rubber-filler gel can be determined experimentally.

The selective wetting of CNTs in NR/IR blend can be calculated according to the following equations:

$$\frac{S^{B(NR)}(t)}{S^{B(IR)}(t)} = \frac{L_P^{IR}}{L_P^{NR}} \cdot \frac{L^{B(NR)}(t)}{L^{B(IR)}(t)} \tag{3}$$

$$S^B = S^{B(NR)}(t) + S^{B(IR)}(t) \tag{4}$$

$S^{B(NR)}$ and $S^{B(IR)}$ are the CNT surface fractions wetted by NR and IR component of blend, respectively. t is the mixing time. S^B is the total filler surface wetted in blend. L_P^{NR}, L_P^{IR} and $L_P^{B(NR/IR)}$ are the saturated rubber content in the gel of the single compounds and blend, respectively. They can be determined from extraction experiments of the samples at a long mixing time.

2.3. Characterization

2.3.1. Vulcanization behavior

Vulcanization kinetics was recorded by means of a Rheometer (Scarabeus) at 150 °C. Vulcanization time t_{90} was determined and used for vulcanization of the mixture.

2.3.2. Optical microscopy

Optical microscopy was used to characterize the CNT macrodispersion. The ratio of the surface of non-dispersed agglomerates to that of the image, A/A_0, is a measure for the filler macrodispersion.

2.3.3. Transmission electron microscopy (TEM)

Ultrathin sections with approximately 50 nm thickness cut from compression-molded plates with a diamond knife (35° cut angle, DIATOME, Switzerland) at −120 °C using a cryo-ultramicrotome RMC PowerTome PT-PC with CRX cryo-chamber (RMC, Tucson) were used for transmission electron microscopy (TEM). The sections were collected on carbon coated copper grids. The specimens were investigated by means of a LEO 912 Omega EFTEM at an accelerating voltage of 120 kV using the zero loss mode.

2.3.4. Raman spectroscopy

The Raman spectroscopy was performed with a Raman spectrometer Holoprobe 785 (Kaiser Optical Systems), which is equipped with a 400 mW diode laser with an excitation wavelength of 785 nm.

2.3.5. Offline conductivity

Measurement of electrical conductivity of cured samples was carried out at room temperature by means of a multimeter 2750 (Fa. Keithley) for high conductive samples and an electrometer 6517A (Fa. Keithley) for low conductive ones.

Tensile test – Stress–strain measurements were performed according to DIN ISO 37 using a tensile tester Z005 (Zwick/Roell) with a cross-head speed of 200 mm min^{-1} at room temperature. The test specimens had a thickness of 1 mm and an initial length of 50 mm. All data presented are the average of five measured specimens for each sample.

2.3.6. Determination of surface energies

Sessile drop contact angle measurements on a sheet of uncured rubbers were conducted with the automatic contact angle meter OCA 40 Micro, DataPhysics Instruments GmbH (Filderstadt, Germany). The surface energies were calculated from the results of these wetting experiments. For this purpose a set of test liquids with different surface tension (and polarity) was used. Surface energy calculations were performed by fitting the Fowkes equation [23].

3. Results and discussion

3.1. Characterization of rubbers investigated

NR was proposed to consist of two trans-1,4 isoprene units, about 1000–3000 cis-1,4 isoprene units with α- and ω-terminal [24–26]. The α-terminal group of NR was postulated to consist of monophosphate and diphosphate groups, which are linked with phospholipids *via* hydrogen bonding as a predominant linkage. On the other hand, the ω-terminal of NR molecule was postulated to be a modified dimethylallyl group linking to a functional group, which is associated with the proteins. Proteins are composed of many types of amino acids, including neutral amino acid, acidic amino acid and basic amino acid. The removal of proteins was mainly made by enzymatic deproteinization of NR with alkali protease in latex stage, which hydrolyzes the protein into water soluble forms [27,28]. After enzymatic deproteinization for 72 h, the nitrogen content of natural rubber was reduced from 0.6 wt% in NR to about 0.08 wt% in DPNR.

The FTIR spectra of the investigated NR, DPNR and IR are presented in Fig. 1a. Both NR and DPNR show a clear peak at 1740 cm^{-1}, which is characteristic for carbonyl group of fatty acid ester of the linked phospholipids. Although the DPNR sample was prepared using ultracentrifugation, the absorbance peak of the carbonyl group in associated fatty acids at 1740 cm^{-1} was still observed in this FTIR spectrum that indicates that the phospholipids are linked to α-terminal of NR chains. In the IR sample, the absorbance peak of carbonyl group at 1740 cm^{-1} disappeared confirming the absence of phospholipids. Three rubbers show clearly a strong peak at 1376 cm^{-1}, which is assigned to scissoring vibration of CH_3 in cis-1,4 units. The peak at 888 cm^{-1} which is attributed to the out-of-plane bending vibration of CH_2 in the $-C{=}CH_2$ (3,4 unit) is strongly observed for IR and weakly for NR and DPNR. Thus, the peaks at 1376 cm^{-1} and 888 cm^{-1} can be used for identification of NR, DPNR and IR in blends by means of FTIR spectra.

Stress–strain curves of the as-received NR, DPNR and IR are shown in Fig. 1b. It is seen that the stress of NR increased strongly

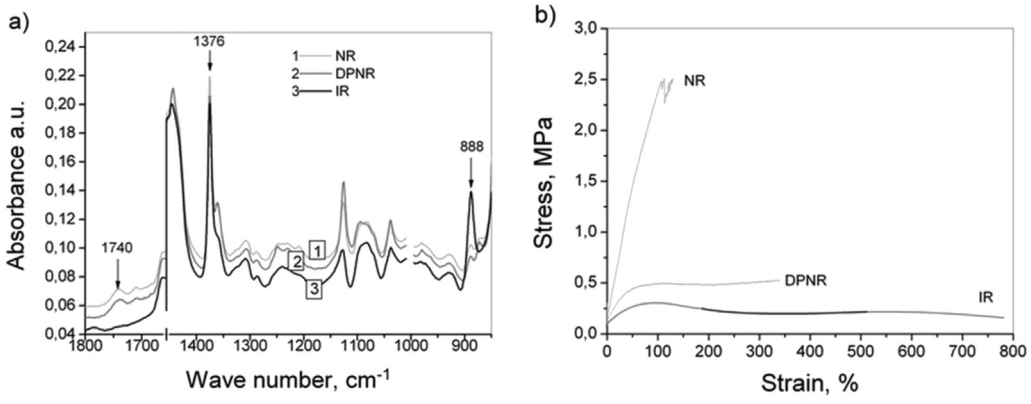

Fig. 1. FTIR spectra (a) and tensile properties (b) of the as-received NR, DPNR and IR.

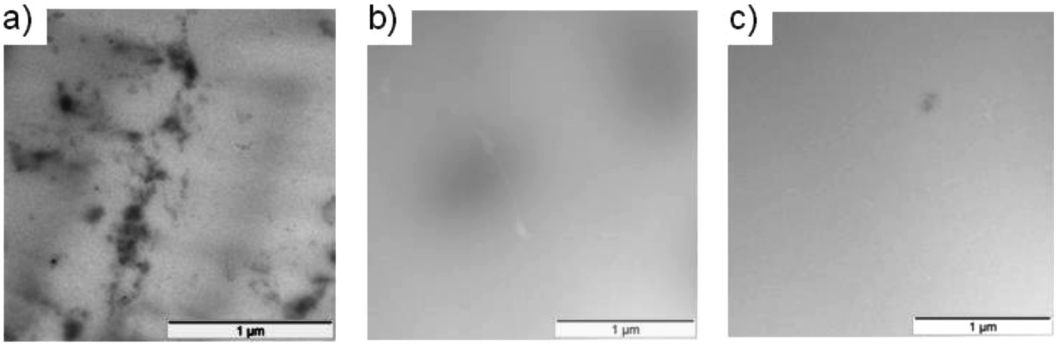

Fig. 2. TEM images of fresh NR (a), DPNR (b) and IR (c).

and reaches a value of 2.5 MPa at a strain of 120%. The low value of strain at break of NR is related to the structural inhomogeneity of the NR due to the presence of non-rubber components. DPNR and IR did not show any increase in stress beyond the strain of 300% during stretching. The difference in the stress–strain behavior under influence of non-rubber components was systematically characterized in several works [29–31]. In general, NR showed higher stress than DPNR and IR in all range of deformation thanks to the presence of the naturally occurring network made up by proteins and phospholipids. The absence of proteins in DPNR and IR clearly destroys the naturally occurring network, resulting in significant decreases in stress properties.

TEM images of the fresh NR, DPNR and IR are shown in Fig. 2. A phase separated structure is found in NR as seen in Fig. 2a, in which bright areas represent natural rubber and dark domains represent non-rubber components. According to Kawahara et al. [29] a membrane layer of protein–lipid complex surrounds the natural rubber particles in latex stage, hence, the non-rubber components may form a separated phase (dark domains) after coagulation of the latex. The phase separated structure of NR vanished after deproteinization due to the removal of the proteins (Fig. 2b). A clean image can be observed for IR as seen in Fig. 2c because of the absence of any non-rubber component in this synthetic rubber.

Gel formation in fresh NR, DPNR and IR was investigated by storing rubbers in cyclohexane for seven days. The gel content obtained in NR was 47.0 wt%, in DPNR 1.6 wt% and 0.0 wt% in IR. According to Tarachiwin et al. [24,25] the gel in NR is formed by two types of branching points; the first one is expected to originate from phospholipids, which are associated to rubber chains. The phospholipids are associated together by the formation of micelle structure mainly *via* hydrogen bonding between polar groups in phospholipids molecules. The other branching point is due to proteins, which can be formed *via* hydrogen bonding. Upon deproteinization the gel content is reducing to 1.6 wt% because of the absence of the branching points made by proteins. No gel is formed in IR because of the absence of the branching points. Upon mastication process NR and DPNR showed no gel formation. It is related to the fact that through the compounding the gel structure was destroyed.

3.2. Dispersion of CNTs in NR, DPNR and IR compounds

The online conductance curves of NR, DPNR and IR compound containing 5 phr CNTs are presented in Fig. 3. Without ethanol assistance, three rubbers show no electrical signal (curve 4) that indicates no percolated conductive filler network is formed in rubbers because of the bad filler dispersion. The images made by optical microscopy (Fig. 4a) and TEM (Fig. 4e) show accordingly several large CNT agglomerates in macro and microscopic level, respectively. When CNT/ethanol mixture was added to three rubbers, a significant increase of conductance of several orders of magnitude is observed (curve 2, 3 and 4). It is worthy to note here that the presence of ethanol in ethanol/rubber mixture without any CNTs may show some conductivity signals but they were not detectable in the measuring range of the equipment used. All the online conductance curves show a typical conductance-time characteristics with t_{onset} and t_{Gmax}. At t_{onset} the online conductance starts to rise and reaches the maximum value at t_{Gmax}. According to our previous work [32] the macrodispersion of filler and the online conductance correlate closely to each other. The largest change of the size of filler agglomerates, i.e. the dispersion of large filler agglomerate into smaller aggregates or even individual tubes, is determined in the period between t_{onset} and t_{Gmax}. Upon t_{Gmax} the online conductance decreases that is related to the better distribution of small aggregates throughout the matrix and shortening of tubes as discussed previously [32]. Thus, t_{onset} and t_{Gmax} have often been used for characterization of the filler dispersion kinetics. For IR compound filled with ethanol/CNT paste a t_{onset} recorded at 3 min and t_{Gmax} at 4 min indicate that the dispersion process took place mainly within 1 min related to a fast dispersion of CNTs. Due to the short time of 1 min CNTs had not enough time to be dispersed well in IR matrix. Upon t_{Gmax} the online conductance decays strongly from 8×10^{-2} mS to 5×10^{-5} mS within a mixing interval between 4 min and 10 min. This strong decay of the online conductance means that the main process in this period was the distribution of the large aggregates throughout the IR matrix. The further dispersion of CNTs is suppressed in this mixing period. After

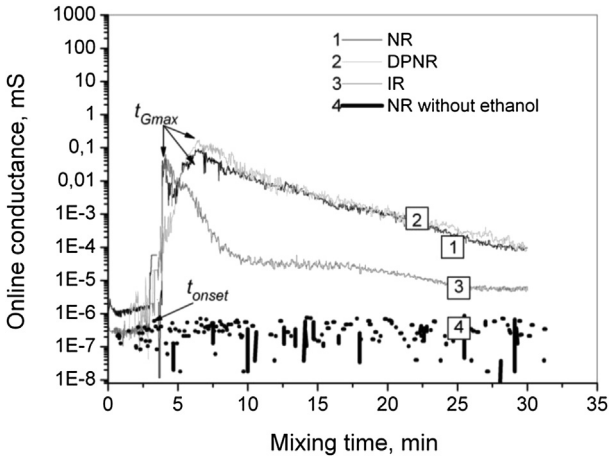

Fig. 3. Online conductance of NR, DPNR and IR compound filled with 5 phr CNTs with assistance of ethanol in dependence on the mixing time.

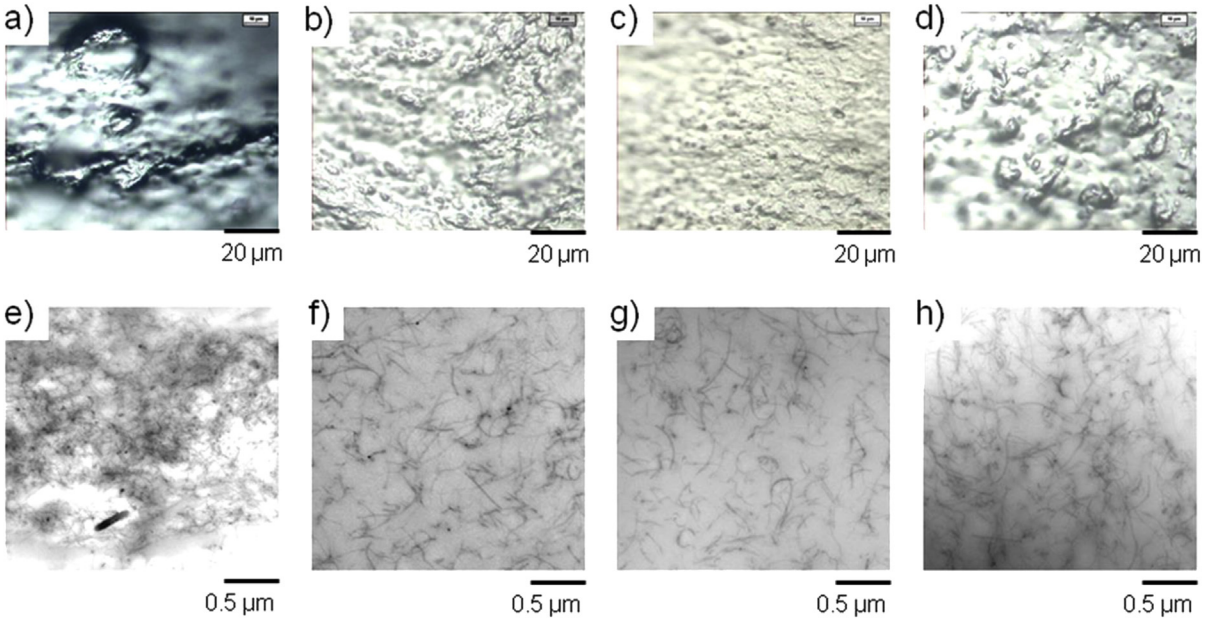

Fig. 4. Optical microscopic images and TEM images of compounds filled with 5 phr CNTs taken out at 30 min mixing time: NR without ethanol a) and e); NR with ethanol b) and f); DPNR with ethanol c) and g); IR with ethanol d) and h).

10 min mixing time the online conductance does not change significant any more that indicates a stationary state of the structure of the IR compound. As a result, the optical macroscopic image of IR compound (Fig. 4d) shows a number of large aggregates ranging from 3 μm to 15 μm. In contrast, NR and DPNR present a similar conductance-time characteristics with a t_{onset} at 3 min and t_{Gmax} at 6 min that indicates a large time interval for dispersion process of both rubbers. Upon t_{Gmax} the online conductance of both compounds decreases gradually, which is different compared to that of IR compounds. According to our previous work [32,33] the online conductance increases with the dispersion process and it decreases with the distribution process. A gradual decrease of the online conductance upon t_{Gmax} is consequently related to the fact that beside the filler distribution as a main process the dispersion process continuously takes place. Thanks to an additional dispersion process taking place at the mixing time after t_{Gmax} the CNT dispersion in NR and DPNR is much better than that in IR as seen in Fig. 4b and c. Although some agglomerates are still observed in NR, DPNR and IR compound with assistance of ethanol, the TEM images of them (Fig. 4e–h) clearly present a very good dispersion of CNTs in microscopic level. Several individual tubes are clearly seen in three compounds that is the reason for their high electrical conductance compared to the samples without ethanol assistance.

3.3. Wetting behavior of CNTs in different rubbers

The wetting kinetics of CNTs in NR, DPNR and IR compound prepared without ethanol is characterized by the rubber layer L in dependence on mixing time (Fig. 5a). The infiltration of NR, DPNR and IR molecules into CNT agglomerate and the dispersion of CNTs take place simultaneously with increasing mixing time according to the *infiltration* model proposed by Manas-Zloczower [34,35]. The rubber layer L of three investigated rubbers increases with different rates and reaches a plateau value after 17 min for NR and DPNR and 100 min for IR. According to our previous work [36], the development of the rubber layer L can be theoretically calculated by Eq. (5).

$$L = \frac{hbt^{1/2}}{hbt^{1/2} + \frac{\rho_E}{\rho_R}(1-\varepsilon)} \tag{5}$$

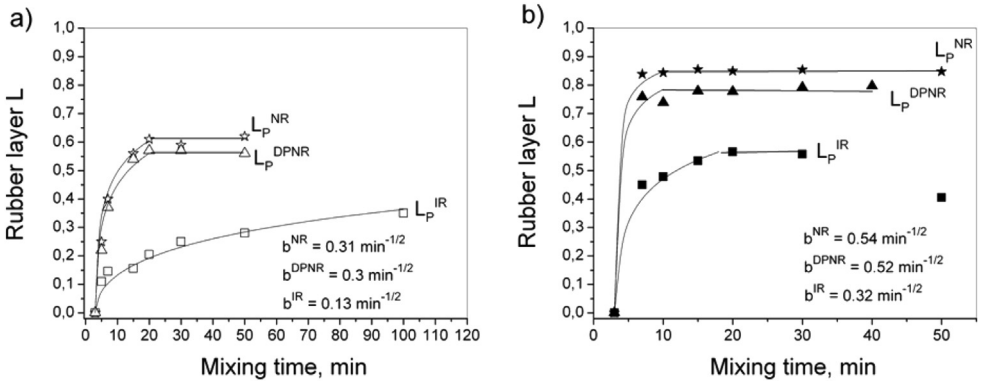

Fig. 5. Rubber layer of NR, DPNR and IR in dependence on mixing time without (a) and with (b) ethanol.

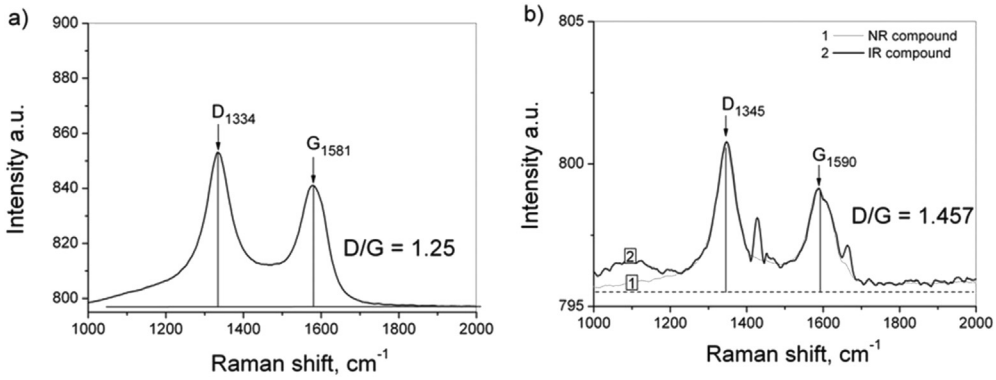

Fig. 6. Raman spectroscopy of the pristine CNTs (a) and CNTs in NR and IR compounds (b).

where ε is the porosity and ρ_F is the density of the filler. ρ_R is the density of rubber. b is a measure for the wetting speed and can be described by Eq. (6):

$$b = \frac{\varepsilon}{D_0}\left(\frac{S\gamma_R \cos\theta}{3\eta_R} + \frac{S^2\Delta P}{6\eta_R}\right)^{1/2} \tag{6}$$

ΔP is the pressure in the mixing chamber, S is considered as pore size of filler. γ_R is the surface tension of rubber, θ is the contact angle and η_R is the rubber viscosity. D_0 is the average agglomerate diameter. The correlation between the plateau value L_P and the factor h can be described by Eq. (7):

$$L_P = \frac{\varepsilon h}{\varepsilon h + \frac{\rho_F}{\rho_R}(1-\varepsilon)} \tag{7}$$

By fitting Eq. (5) to the experimental data presented in Fig. 5a with $\rho_R = 0.94$ g/cm^3 and $\rho_F = 2.0$ g/cm^3, $\varepsilon = 0.92$ [37,38] the wetting speed $b^{NR} = 0.31$ min$^{-1/2}$ and $b^{DPNR} = 0.3$ min$^{-1/2}$ and $b^{IR} = 0.13$ min$^{-1/2}$ can be experimentally determined for NR, DPNR and IR, respectively. It is clear that NR and DPNR show the similar wetting behavior. It lets us conclude that the absence of proteins does not influence the wetting kinetics of CNTs. However, if the phospholipids are not present the CNT wetting speed is strongly decreased as seen in the case of IR.

By mixing CNTs into rubbers with assistance of ethanol the rubber layer L increases faster as seen in Fig. 5b. According to Fig. 3 ethanol accelerates the CNT dispersion process, thus, it eases the rubber-filler contact and consequently speeds up the wetting. As a result, $b^{NR} = 0.54$ min$^{-1/2}$, $b^{DPNR} = 0.52$ min$^{-1/2}$ and $b^{IR} = 0.32$ min$^{-1/2}$ were determined for three investigated rubbers. In this case, DPNR is similar to NR with respect to the CNT wetting behavior. IR wets CNTs slower than the other rubbers even with assistance of ethanol.

According to Eq. (6) the wetting speed b increases with increasing rubber surface tension. By means of the contact angle measurement the surface tension $\gamma_{NR} = 22$ mN/m of NR and $\gamma_{IR} = 20$ mN/m of IR were determined. The insignificant difference in surface tension of both rubbers cannot explain the significant difference in wetting behavior between NR and IR. It needs further investigation regarding the rubber-filler interactions.

Raman investigation of CNT filled NR and IR compounds was also performed. In fact, CNTs exhibit well-defined Raman peaks located at 1334 cm^{-1} assigned to the disordered graphite structure (D band), and at 1581 cm^{-1} related to the tangential stretching mode of carbon–carbon bonds (G band) as shown in Fig. 6a. The intensity of all peaks was normalized to yield the same intensity for the G-band.

A shift of D and G-band of CNTs filled in NR (D: 1345 cm^{-1}, G: 1590 cm^{-1}) was observed when compared to the pristine CNTs (Fig 6b). The D/G ratio of CNTs in NR of 1.457 is higher compared to that of the pristine CNTs. This shift and the increase of D/G ratio clearly indicate an interaction between the rubber matrix and the CNT surface and to nanotube–nanotube decoupling within the bundle [39]. As seen in Fig. 6b CNTs in NR and IR show the same spectra. The similarity in spectra of both compounds may reflect the nature of the rubber-filler interactions of CNTs in NR and IR compounds, which are dominantly determined by the Van der Waal bondings between isoprene backbone and CNT surface. Because of the small

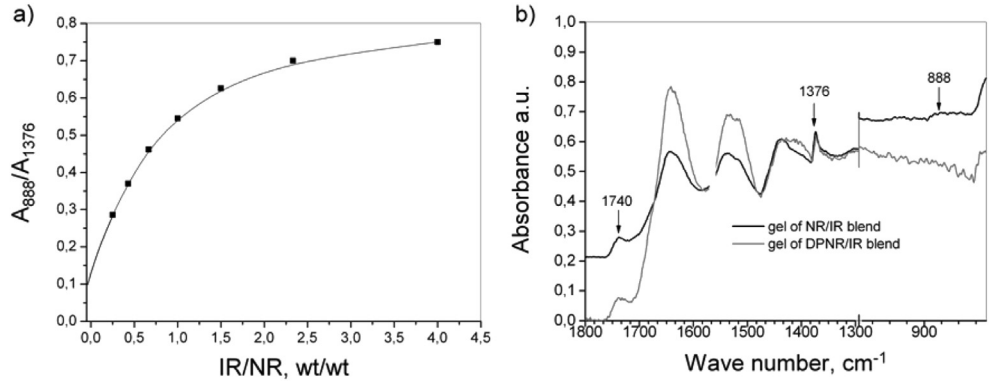

Fig. 7. Correlation between the surface ratio A_{888}/A_{1376} and the mass ratio IR/NR (a), FTIR spectra of the rubber-filler gels of NR/IR and DPNR/IR blend (b).

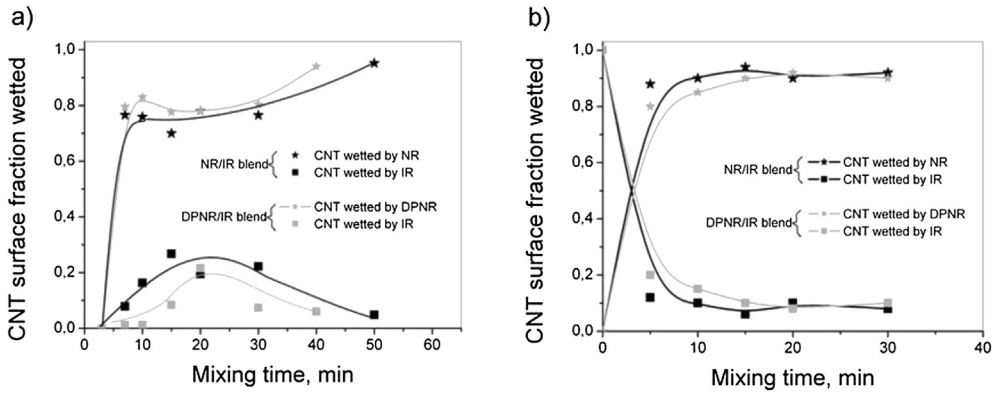

Fig. 8. Selective wetting of CNTs in statistic blends NR/IR and DPNR/IR (a) as well as masterbatch blends NR/(IR-CNT) and DPNR/(IR-CNT) (b) in dependence on mixing time.

quantity of phospholipids and proteins the influence of the cation-π interaction is not clearly detectable by Raman.

3.4. Selective wetting of CNTs in NR/IR and DPNR/IR blends

In order to compare the rubber-filler affinity of CNTs to different rubbers directly, CNTs were mixed into 50/50 NR/IR and DPNR/IR blend. The preferential wetting of CNT surface by a blend component can be a measure for the better rubber-filler interaction of CNTs to this rubber. For creation of the calibration curve, blends with different mass ratios NR/IR and DPNR/IR were prepared and investigated by FTIR. The correlation between the area peak ratio A_{888}/A_{1376} and the given mass ratio IR/NR presented in Fig. 7a is not described by a straight line as we often observed for other systems reported in our previous works [20–22]. Thus, the ratio $L^{B(IR)}/L^{B(NR)}$ in the rubber-filler gel can be determined manually using the calibration curve presented in Fig. 7a. In Fig. 7b spectra of the rubber-filler gels of NR/IR and DPNR/IR blend are shown. Due to the extraction process by cyclohexane the unbound rubber was extracted and thus, in the rubber-filler gel only the rubber components bonded to CNT surface are present. It is clear that the peak at 888 cm^{-1}, which is mainly characteristic for IR phase disappears in both spectra, i.e. IR component is entirely extracted from the blends. In contrast, the absorbance peak at 1740 cm^{-1} of phospholipids of NR and DPNR phase appears in both spectra confirming the presence of bound NR and DPNR in the gel.

The kinetics of CNT wetting in statistic blends NR/IR and DPNR/IR was experimentally characterized by the *wetting concept* according to Eqs. (3) and (4). As seen in Fig. 8a the CNT surface fractions $S^{B(NR)}$ and $S^{B(IR)}$ wetted by NR and IR phase, respectively, increase immediately after adding 5 phr CNT into NR/IR blend. It is clear that NR wets more CNTs than IR in the first mixing stage (up to 20 min) due to the higher wetting speed as observed in Fig. 5. A CNT fraction of 0.75 was found to be wetted by NR and 0.25 by IR phase at 20 min mixing time. In the second mixing stage from 20 min to 50 min, the fraction $S^{B(NR)}$ gradually increases, while $S^{B(IR)}$ decreases. This result is attributed to the CNT transfer process from the IR to NR phase as a result of the replacement of IR on the CNT surface by NR. CNT transfer is obviously owing to the higher affinity of CNTs to NR than to IR. At 50 min mixing time a CNT surface fraction of 0.95 is wetted by NR, while IR wets only a surface fraction of 0.05.

Fig. 8b shows really the replacement process of IR by NR molecules on the CNT surface when mixing CNT/IR masterbatch with

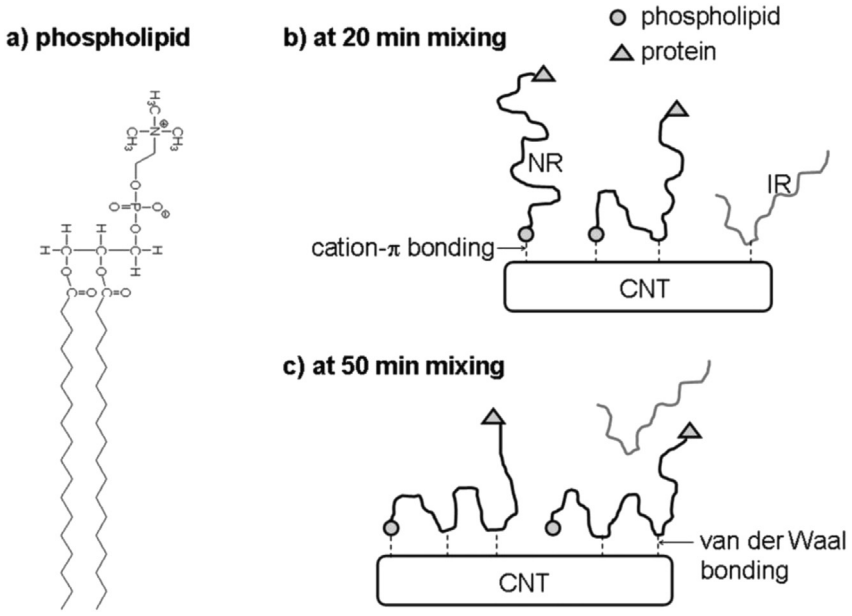

Fig. 9. Chemical structure of phospholipid (a) and proposed filler–rubber interactions in CNT/NR composite (b,c).

the fresh NR. At the beginning of the mixing process CNT surface was entirely wetted by IR. After 5 min mixing 90% of bound IR was replaced by NR molecules.

The selective wetting of CNTs in DPNR/IR blends is presented also in Fig. 8. The deproteinization has clearly no effect on the affinity of natural rubber to CNTs. Thus, it can be concluded that only the presence of phospholipids is essential for the rubber-filler interaction of CNTs in NR. When CNTs are mixed into NR, the ammonium cation N^+ of phospholipids can interact with CNT surface *via* cation–π interaction forming stable linkages beside the Van der Waals bondings. The cation–π interaction was proposed by Ma and Fukushima et al. [40–42] as main linkage between CNTs and ionic liquid. In Fig. 9a and b the chemical structure of phospholipid and the proposed adsorption of NR molecules on CNT surface *via* cation-π linkage and Van der Waals bonding are illustrated, respectively. Based on the experimental result shown in Fig. 8 it can be postulated that NR and IR wet CNTs simultaneously in the first mixing period up to 20 min mixing time, however, about 75% of CNT surface is wetted by NR because of the presence of phospholipids. The phospholipids act as anchor points firmly bonding NR terminal with CNT surface. With increasing mixing time NR molecule can enhance its interaction with CNTs through Van der Waal bondings between its backbone and CNT surface as illustrated in Fig 9b. Through its conformational rearrangement and thermodynamic driving forces NR molecules gradually replace IR molecules on the CNT surface in the second period from 20 min to 50 min mixing time until CNT surface is entirely wetted by NR molecules (Fig. 9c).

On the basis of the *Z-model* proposed in our previous work [20] the selective filler wetting in a binary NR/IR blend at a thermodynamic equilibrium state can be predicted using Eqs. (8) and (9).

$$\frac{S_{eq}^{B(NR)}}{S_{eq}^{B(IR)}} = n_{NR/IR}\left(\frac{\gamma_{IR}+\gamma_F-2\sqrt{\gamma_{IR}\gamma_F}}{\gamma_{NR}+\gamma_F-2\sqrt{\gamma_{NR}\gamma_F}}\right)^2 \quad (8)$$

$$S^B = S_{eq}^{B(NR)} + S_{eq}^{B(IR)} \quad (9)$$

$S_{eq}^{B(NR)}$ and $S_{eq}^{B(IR)}$ are the filler surface fractions wetted by NR and IR phase at an equilibrium state. $n_{NR/IR}$ is the mass ratio of the rubber phase NR to IR. γ_{NR}, γ_{IR} and γ_F are the surface tension values of the blend components and filler, respectively. S^B is the total filler surface added to the blend. For an entire wetting of CNT surface S^B is equal to unity. Setting the surface tension values $\gamma_{NR} = 22$ mN/m and $\gamma_{IR} = 20$ mN/m of rubber components into Eqs. (8) and (9) with $n_{NR/IR} = 1$ for 50/50 NR/IR blend, a *Z*-shaped master curve (curve 1) demonstrating the filler surface fraction wetted by NR phase in dependence on filler surface tension can be created as seen in Fig. 10. Fitting the CNT surface tension $\gamma_F = 30$ mN/m [20,21] into the master curve a CNT surface fraction wetted by each phase, $S_{eq}^{NR} = 0.76$ and $S_{eq}^{IR} = 0.24$, respectively can be predicted for thermodynamic equilibrium state.

By comparing the prediction with the experimental result shown in Fig. 8 it is clear that the prediction under-estimated the CNT surface fraction wetted by NR $S^{B(NR)}$. The mismatch of the prediction may be related to the fact that the surface tension value of NR used for prediction was determined by the contact angle measurement. Because the content of the phospholipids is very small (<1 wt%) and they are linked to the terminal of NR, i.e. they cannot migrate to the surface of the rubber sample. Thus, the surface tension is determined merely by the isoprene backbone.

In order to quantify the effect of phospholipids on the CNT wetting the value of the surface tension of NR is stepwise increased by keeping constant the surface tension of IR and CNTs. The

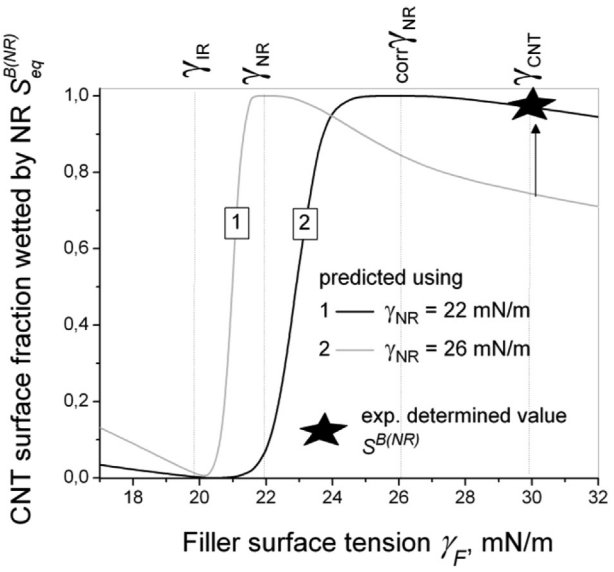

Fig. 10. Master curves of filler wetting in dependence on filler surface tension.

obtained master curve is correspondingly changed in direction indicated by the arrow shown in Fig. 10. When the predicted $S_{eq}^{B(NR)}$ reaches the experimentally determined value $S^{B(NR)}$ of 0.95 (curve 2), the surface tension of NR reaches the values ranging from 25.5 mN/m to 26.5 mN/m. Thus, the effect of phospholipids on the NR-CNT interaction can be quantitatively described by the corrected value of the surface tension of NR, corr $\gamma_{NR} = 26$ mN/m, which is well corresponding to those determined from other systems [21].

3.5. Effect of the CNT wetting on the vulcanization kinetics and conductivity as well as tensile properties of filled compounds

The vulcanization kinetics of fresh compounds of NR, DPNR and IR filled with CNTs recorded at 150 °C is shown in Fig. 11a. IR shows the longest t_{onset} of vulcanization. The presence of phospholipids in DPNR accelerates the vulcanization significantly. The t_{onset} is reduced to 3.5 min. Both phospholipids and proteins in NR decrease the t_{onset} to 2 min. The effect of non-rubber components on the vulcanization kinetics of the unfilled NR and deproteinized NR was also found by Wang et al. [43]. They stated that phospholipids and proteins may promote the formation of vulcanization intermediates or crosslink precursors in the initial stage of NR vulcanization. It is obvious in Fig. 11a that before the t_{onset} is reached the torque of filled NR and DPNR is the same and lower than that of the IR compound. The high value of torque of IR compound may be related to the strong re-aggregation of the individual tubes. According to the work made by Wang et al. [44,45] and Stöckelhuber et al. [46] the re-aggregation or flocculation of the dispersed filled aggregates can take place after mixing at high temperature. The extent of the filler flocculation is determined by the competition between filler–filler affinity and rubber-filler affinity. In the present work, the filler–filler affinity in three systems is the same, thus, the flocculation is merely determined by the rubber-filler affinity. Based on the values of the rubber layer of NR, DPNR and IR shown in Fig. 5 it can be postulated that the tube–tube distance of the CNT network in IR compound is shorter than that in other compounds. The shorter tube–tube distance can consequently eases the re-aggregation of CNTs in IR. Moreover, the interfacial tension value $\gamma_{NR\text{-}CNT}$ of 0.14 mN/m and $\gamma_{IR\text{-}CNT}$ of 1.01 mN/m of NR and DPNR compounds, respectively which are a

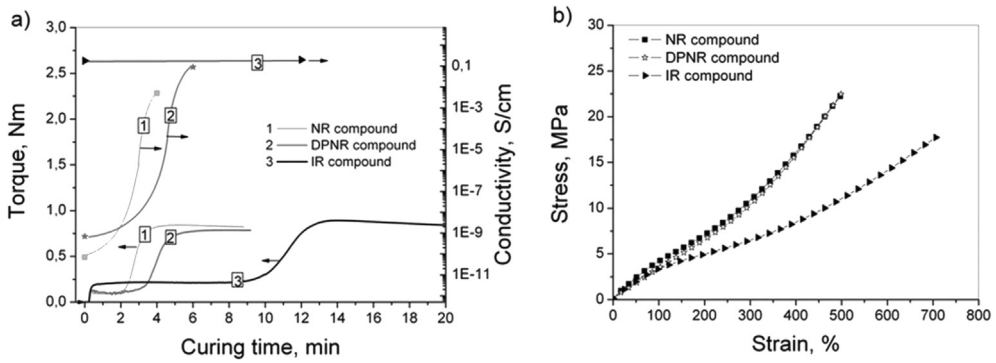

Fig. 11. Vulcanization curves and offline conductivity (a) and stress–strain curves (b) of filled NR, DPNR and IR compounds.

measure for rubber-filler interaction, were calculated by taking into consideration the corrected value corr. $\gamma_{NR} = 26$ mN/m. The lower value of $\gamma_{NR\text{-}CNT}$ indicates that the affinity of CNTs to NR is better than to IR which was evidenced by the selective wetting of CNTs in NR/IR blend (Fig. 8). The strong rubber-filler interaction hinders the re-aggregation or flocculation of individual CNTs in NR and DPNR compounds. The flocculation of CNTs in IR compound collected just after mixing is the reason for the high value of the offline conductivity of IR as seen in Fig. 11a. In contrast, the poor filler network in NR and DPNR causes a very low value of the offline conductivity of NR and DPNR compounds. The flocculation of CNTs in NR and DPNR can be promoted at high temperature during vulcanization. Through this flocculation process the offline conductivity of NR and DPNR increases strongly and approaches that of IR as seen in Fig. 11a.

Stress–strain curves of filled NR, DPNR and IR vulcanizates are shown in Fig. 11b. It is visible that the stresses of three vulcanizates are the same in the strain interval up to 70%. It is well-known that in the small deformation the contribution of filler network to the total stress is dominant. The similar CNT network in the vulcanized state of three samples is the reason for the same stress of them shown in Fig. 11b and for the same values of the offline conductivity shown in Fig. 11a. Beyond the strain of 70% the filler network is destroyed, however, the stress of NR and DPNR increased significantly, while the stress of IR increases only moderately. According to the work made by Amnuaypornsri et al. [30] the strain induced crystallization and the related enhancement of stress were observed at strain higher than 300%. This implies that the improvement of stress beyond the strain of 70% observed in the present work is not determined by the strain induced crystallization but it is rather caused by the better rubber-filler interaction of CNTs in NR and DPNR thanks to the presence of the phospholipids.

4. Conclusions

In the present work the effect of the linked phospholipids of NR on the rubber-filler interactions was investigated. NR, DPNR and IR were used as matrix for CNTs. The selective wetting of CNTs in miscible NR/IR and DPNR/IR blends was investigated by means of the *wetting concept* based on FTIR analysis of the rubber-filler gel of blends. It revealed that the surface of CNTs is entirely wetted by NR or DPNR molecules, respectively, but not by IR. This result emphasizes that proteins do not influence the affinity between NR and CNTs, while the linked phospholipids interact with CNT surface through cation-π interaction. This linkage acts as an anchor point helping NR molecules to wet CNT surface dominantly. The effect of phospholipids on the vulcanization kinetics, electrical and mechanical properties was also discussed by taking into consideration the cation-π interaction. The modified *wetting concept* presented in this work can be used for characterization of selective wetting of different fillers in blends consisting of miscible rubber components. It opens a new possibility for direct comparison of two similar and/or miscible rubbers regarding their rubber-filler interactions.

Acknowledgments

The authors wish to thank the Deutsche Forschungsgemeinschaft (DFG) (Project Nr. LE 3202/1-1) for the financial support.

References

[1] Rajan VV, Dierkes WK, Joseph R, Noordermeer JWM. Prog Polym Sci 2006;31:811–34.
[2] Park SM, Lim YW, Kim CH, Kim DJ, Moon WJ, Kim JH, et al. J Ind Eng Chem 2013;19:712–9.
[3] Rattanasom N, Prasertsri S. Polym Test 2003;28:270–6.
[4] Zhou XW, Zhu YF, Liang J. Mater Res Bull 2007;42:456–64.
[5] Liu Y, Li L, Wang Q, Zhang X. J Polym Res 2011;18:859–67.
[6] Bokobza L, Rahmani M, Belin C, Bruneel J-L, El Bounia N-E. J Appl Polym Sci 2008;46:1939–51.
[7] Bokobza L. Polymer 2007;48:4907–20.
[8] Ismail H, Ramly F, Othman N. Polym Plast Technol Eng 2010;49:260–6.
[9] Sui G, Zhong WH, Yang XP, Yu YH. Mater Sci Eng 2008;485:524–31.
[10] Fakhrul-Razi A, Atieh MA, Girun N, Chuah TG, El-Sadig M, Biak DRA. Comp Struct 2006;75:496–500.
[11] Bokobza L. eXPRESS Polym Let 2012;6(3):213–23.
[12] Kolodziej M, Bokobza L, Bruneel J-L. Comp Interf 2007;14:215–28.
[13] Movahed SO. Nanofiller in tire tread: It's benefit for tire performance. VDM Verlag Dr. Müller; 2010. ISBN: 13: 978-3639099416.
[14] Boonmahitthisud A, Chuayjuljit S. Adv Mater Res 2011;347–353:3197–200.
[15] Boonmahitthisud A, Chuayjuljit S. J Met Mater Min 2012;22:77–85.
[16] Kueseng P, Sae-oui P, Rattanasom N. Polym Test 2013;32:731–8.
[17] Kueseng P, Sae-oui P, Sirisinha Ch, Jacob K, Rattanasom N. Polym Test 2013;32:1229–36.
[18] Thomas SP, Thomas S, Mathew EJ, Marykutty CV. Polym Comp 2013. http://dx.doi.org/10.1002/pc.22740.
[19] Yan N, Xia HS, Zhan YH, Fei GX, Chen C. Plast Rubber Comp 2012;41:365–72.
[20] Le HH, Parsekar M, Ilisch S, Henning S, Das A, Stöckelhuber K-W, et al. Macromol Mater Eng 2013. http://dx.doi.org/10.1002/mame.201300254.
[21] Le HH, Sriharish MN, Henning S, Klehm J, Menzel M, Frank W, et al. Comp Sc Technol 2014;90:180–6.
[22] Le HH, Ilisch S, Heidenreich D, Wutzler A, Radusch H-J. Polym Comp 2010;31:1701–11.
[23] Fowkes FM. J Phys Chem 963;67:2538–41.
[24] Tarachiwin L, Sakdapipanich JT, Ute K, Kitayama T, Bamba T, Fukusaka E. Biomacromolecules 2005;6:1851–7.
[25] Tarachiwin L, Sakdapipanich J, Ute K, Kitayama T, Tanaka Y. Biomacromolecules 2005;6:1858–63.
[26] Tanaka Y, Mori M, Ute K, Hatada K. Rubber Chem Technol 1990;63:1–7.
[27] Eng AH, Tanaka Y, Gan SN. J Nat Rubber Res 1992;7:152–5.
[28] Tarachiwin L, Sakdapipanich J, Tanaka Y. Kautsch Gummi Kunstst 2005;58:115–22.
[29] Kawahara S, Chaikumpollerta O, Akabori K, Yamamoto Y. Polym Adv Technol 2011;22:2665–7.

[30] Amnuaypornsri S, Sakdapipanich J, Toki S, Hsiao BS, Ichikawa N, Tanaka Y. Rubber Chem Technol 2008;81:753–66.
[31] Nawamawat K. Effect of non-rubber components on basic characteristics and physical properties of natural rubber from hevea brasiliens. Phd thesis. Thailand: Mahidol University; 2008.
[32] Le HH, Hoang XT, Das A, Gohs U, Stöckelhuber K-W, Boldt R, et al. Carbon 2012;50:4543–56.
[33] Le HH, Ilisch S, Steinberger H, Radusch H-J. Plast Rubber Compos: Macromol Eng 2008;37:367–75.
[34] Li Q, Feke DL, Manas-Zloczower I. Rubber Chem Technol 1995;68:836.
[35] Manas-Zloczower I. Rheol Bull 1997;66:5.
[36] Le HH, Keller M, Hristov M, Ilisch S, Hoang TX, Do QK, et al. Macromol Mater Eng 2013;298:1083–99.
[37] Puretzky AA, Geohegan DB, Ivanov JIN. Appl Phys A 2005;81:223–40.
[38] Wang T, Jeppson K, Liu J. Carbon 2010;48:3795–801.
[39] Bokobza LJ. Inorg Org Polym Mater 2012;22:629–35.
[40] Ma JC, Dougherty DA. Chem Rev 1997;97:1303–24.
[41] Fukushima T, Kosaka A, Ishimura Y, Yamamoto T, Takigawa T, Ishii N. Science 2003;300:2072–4.
[42] Fukushima T, Aida T. Chem Eur J 2007;13:5048–58.
[43] Wang PY, Wang YZ, Zhang BL, Huang HH. J Appl Polym Sci 2012;126:1183–7.
[44] Wang M-J. Rubber Chem Technol 1998;71:520–89.
[45] Wang M-J. Kautsch Gummi Kunstst 2007;60:438–43.
[46] Stöckelhuber KW, Svistkov A, Pelevin A, Heinrich G. Macromolecules 2011;44:4366–81.